

RESEARCH PAPER



CXADR promote epithelial–mesenchymal transition in endometriosis by modulating AKT/GSK-3 β signaling

Hang-Jing Tan^{a,b}, Zi-Heng Deng^{a,b}, Chun Zhang^c, Hong-Wen Deng^d, and Hong-Mei Xiao^{a,b}

^aInstitute of Reproduction and Stem Cell Engineering, School of Basic Medical Science, Central South University, Changsha, China; ^bCenter for Reproductive Health, and System Biology, Data Sciences, School of Basic Medical Science, Central South University, Changsha, China; ^cDepartment of Gynaecology and Obstetrics, Xiangya Hospital, Central South University, Changsha, China; ^dCenter of Biomedical Informatics and Genomics, Deming Department of Medicine, Tulane University School of Medicine, New Orleans, LA, USA

ABSTRACT

Endometriosis is a benign high prevalent disease exhibiting malignant features. However, the underlying pathogenesis and key molecules of endometriosis remain unclear. By integrating and analysis of existing expression profile datasets, we identified coxsackie and adenovirus receptor (CXADR), as a novel key gene in endometriosis. Based on the results of immunohistochemistry (IHC), we confirmed significant down-regulation of CXADR in ectopic endometrial tissues obtained from women with endometriosis compared with healthy controls. Further *in vitro* investigation indicated that CXADR regulated the stability and function of the phosphatases and AKT inhibitors PHLPP2 (pleckstrin homology domain and leucine-rich repeat protein phosphatase 2) and PTEN (phosphatase and tensin homolog). Loss of CXADR led to phosphorylation of AKT and glycogen synthase kinase-3 β (GSK-3 β), which resulted in stabilization of an epithelial–mesenchymal transition (EMT) factor, SNAIL1 (snail family transcriptional repressor 1). Therefore, EMT process was induced, and the proliferation, migration and invasion of Ishikawa cells were enhanced. Over-expression of CXADR showed opposite effects. These findings suggest a previously undefined role of AKT/GSK-3 β signaling axis in regulating EMT and reveal the involvement of a CXADR-induced EMT, in pathogenic progression of endometriosis.

ARTICLE HISTORY

Received 15 August 2022
Revised 6 December 2023
Accepted 12 December 2023

KEYWORDS



Endometriosis; CXADR, EMT; AKT-signaling pathway


1. Introduction

Endometriosis, characterized by dysmenorrhea, pelvic pain and infertility, is a common and refractory gynecological disorder [1–4]. It is a benign disease resembling malignancies to some extent, including invasive, progressive and estrogen-dependent growth, greatly influencing the physical and mental health of affected women [5,6]. The widely accepted theory of Sampson proposes that endometriosis originates from retrograde menstruation of endometrial tissue entering the abdominal cavity through the fallopian tubes [7]. However, only 10%–15% of women develop endometriotic disease, whereas 90% of women suffer from retrograde menstruation [8], indicating that other cellular and molecular events contribute to the development of endometriosis but they remain largely unclear.

Bioinformatics tools, which can collate vast amounts of information about gene expression and gene function, have been used to explore pathogenesis or improve the diagnosis of numerous diseases, such as colorectal cancer, lung adenocarcinoma and prostate cancer [9–11]. In this study, we mined and integrated three publicly available human endometrial microarray datasets, revealing coxsackie and adenovirus receptor (CXADR), which was down-regulated in ectopic endometrium compared to normal endometrium, to be a novel potentially gene in promoting development of endometriosis.

CXADR-mediated formation of an AKT-inhibitory signalosome at tight junctions (TJs) [12]. TJs regulate epithelial proliferation, polarization, and differentiation [13]. Deregulation of TJs is a hallmark of epithelial – mesenchymal transition (EMT), which is characterized by decreased

CONTACT Hong-Mei Xiao  hmxiao@csu.edu.cn  Institute of Reproduction and Stem Cell Engineering, School of Basic Medical Science, Central South University, Xiangya Road Xiangya Medical College, Kaifu District, Changsha, Hunan Province 410000, China

 Supplemental data for this article can be accessed online at <https://doi.org/10.1080/15384101.2023.2296242>

expression of epithelial markers and tight junction proteins, such as E-cadherin and claudins, respectively, and increased expression of mesenchymal markers, such as vimentin [14]. Migration and invasion are therefore enhanced, which is a prerequisite for the establishment of endometriotic lesions [15–18]. Specifically, in breast cancer, loss of CXADR led to the instability of PTEN and PHLPP2, and TJs were deregulated. PTEN and PHLPP2 are AKT inhibitors, so instability of PTEN and PHLPP2 causes phosphorylation of AKT. Glycogen synthase kinase-3 β (GSK-3 β) is a downstream target of AKT, which in its active state targets the EMT factor SNAIL1 (snail family transcriptional repressor 1). Therefore, phosphorylation of AKT resulted in phosphorylation of GSK-3 β and stabilized SNAIL1, and thus EMT was induced [12]. However, the role of CXADR, and AKT/GSK-3 β -Snail/signaling axis, in endometriosis remains unclear.

Accordingly, in this study, we aimed to investigate the role of CXADR in endometriosis *in vitro*, which may aid in developing suitable therapeutic strategies.

2. Materials and methods

2.1 Study design

The study design is shown in Figure 1. In our current research, three datasets, including GSE7305, GSE25628 and GSE58178 were extracted

from Gene Expression Omnibus (GEO) database (<https://www.ncbi.nlm.nih.gov/geo>). Three datasets contained ectopic endometrium of endometriosis patients and endometrium of healthy controls. In each dataset, differentially expressed genes (DEGs) were screened, and hub genes were identified by Weighted Gene Co-expression Network Analysis (WGCNA). Common DEGs in GSE7305, GSE58178, GSE25628 were selected to form Dataset 1. Common hub genes identified by WGCNA in GSE7305, GSE58178, GSE25628 were selected to form Dataset 2. Common genes in Dataset 1 and Dataset 2 were selected as final key gene, and we identified CXADR as a novel key gene in endometriosis. Then the *in vitro* functional verification, such as immunohistochemistry (IHC) for clinical samples, and related cell and molecular experiments for CXADR were carried out.

2.2 Microarray data

GSE7305 contained ectopic endometrium of 10 endometriosis patients and endometrium of 10 healthy controls, and the dataset was based on GPL570 (Affymetrix Human Genome U133 Plus 2.0 Array) [19]. GSE58178 contained ectopic endometrium of six endometriosis patients and endometrium of six healthy controls, and the dataset was based on GPL6947 (Illumina HumanHT-12 V3.0 expression beadchip) [20]. GSE25628 contained ectopic endometrium of eight

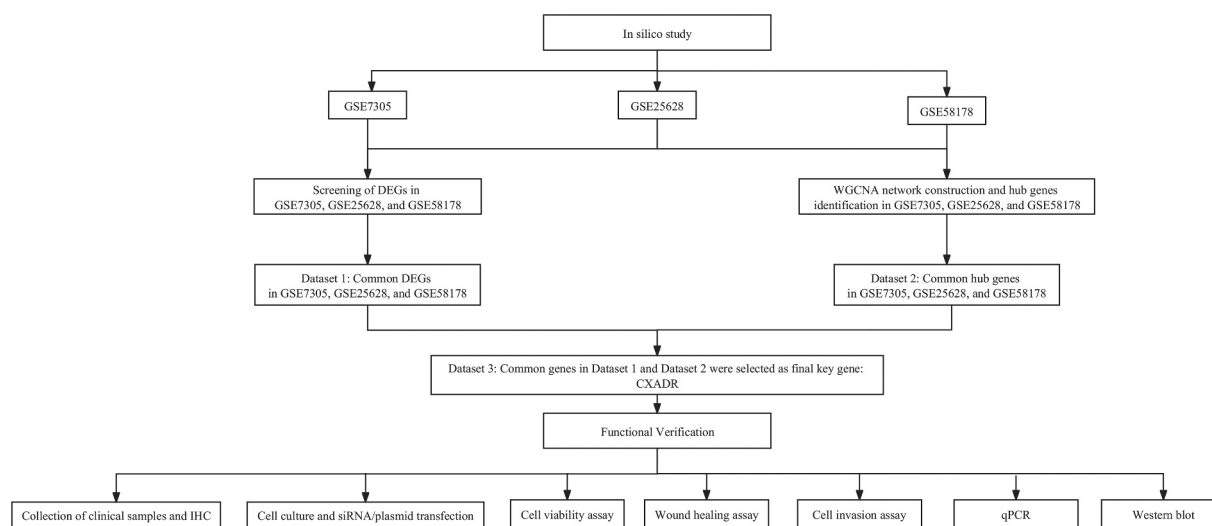


Figure 1. Study design. DEGs: differentially expressed genes. WGCNA: weighted gene co-expression network analysis. IHC: immunohistochemistry.

endometriosis patients and endometrium of six healthy controls, and the dataset was based on GPL571([HG-U133A_2] Affymetrix Human Genome U133A 2.0 Array) [21]. The patients for microarray analysis suffer from endometriomas or deep infiltrating endometriosis.

2.3 Data processing and differentially expressed genes (DEGs) identification

These three raw datasets were analyzed by GEO2R (<https://www.ncbi.nlm.nih.gov/geo/geo2r/>), which is an online tool employed to compare two or more samples in different datasets. Genes that satisfied adjust P-value <0.05 and $|\logFC| >2$ were defined as DEGs, and common DEGs in GSE7305, GSE58178, GSE25628 were selected to form Dataset 1.

2.4 Weighted gene co-expression network analysis (WGCNA) network construction and key genes identification

Weighted Gene Co-expression Network Analysis (WGCNA) can be used for finding clusters (modules) of highly correlated genes and for relating modules to sample trait (endometriosis) [22]. Correlation networks facilitate network-based gene screening methods that can be used to identify candidate biomarkers or therapeutic targets [22]. We used the WGCNA R package to construct the coexpression network in each datasets (GSE7305, GSE58178, and GSE25628). First, we constructed a gene co-expression by R function `pickSoftThreshold` and calculated the soft thresholding power β . Second, we identified the genes clusters (modules) by hierarchical clustering and the dynamic tree cut function. Modules were displayed in different colors. Third, module-trait associations were estimated using the correlation between the module eigengene and the trait. Fourth, the absolute value of gene significance (GS) and module membership (MM) of each gene, in the module which most positive or negative related to endometriosis, were calculated. GS refers to the Pearson correlation coefficients between the expression levels of each gene and each clinical trait [23]. MM refers to the absolute value of the Pearson's correlation between the gene

and the eigengene [24]. Fifth, genes in each dataset with a GS over 0.6 and an MM over 0.8 in the most trait-relevant module were selected as hub genes. Sixth, common hub genes in GSE7305, GSE58178, GSE25628 were selected to form Dataset 2. Last, common genes in Dataset 1 and Dataset 2 were selected as final key genes.

2.5 Clinical specimens

Patients undergoing laparoscopy for endometriosis were recruited from the Department of Pathology, Xiangya Hospital, Central South University. In this study, 15 ovarian chocolate cyst (endometriotic tissue samples), and 10 samples of normal endometrium in patients with cervical intraperitoneal neoplasia (CIN) III, were used for immunohistochemical (IHC) analysis. All patients had regular menstrual cycles (21–35 days), and none had received any hormone therapy for at least 3 months prior to the operation. All samples were collected during the proliferative phase of the menstrual cycle, as confirmed by both the date of the last menstrual period and histological diagnosis. Clinical characteristics of the patients and tissues used in the present study are shown in Supplementary materials.

2.6 Cell culture

Ishikawa cell line was purchased from Fenghui Biotechnology Co., Ltd (Hunan, China) and cultured in modified Eagle's medium with 15% fetal bovine serum and 100 IU/mL penicillin (BasalMedia, Shanghai, China) in a humidified atmosphere with 5% CO₂ at 37°C. EMT was induced by the addition of TGF β (Peprotech, NJ, USA) at doses of 10 ng/mL for designated time.

2.7 Immunohistochemistry (IHC)

To validate the expression levels of CXADR, PHLPP2, PTEN and SNAIL1 in endometriosis, IHC was performed on paraffin-embedded tissue sections as described previously [25]. The primary antibodies used in the present study were rabbit polyclonal anti-CXADR (1:100; Affinity, MI, USA), rabbit polyclonal anti-PHLPP2 (1:100, Proteintech, Wuhan, China), rabbit polyclonal anti-SNAIL1 (1:100, Proteintech, Wuhan, China),

rabbit polyclonal anti-E-cadherin (1:200, Huaan, Hangzhou, China), rabbit polyclonal anti-vimentin (1:200, Immunoway, TX, USA), rabbit polyclonal anti-claudin-4 (1:400, Abcam, Cambridge, UK), and mouse monoclonal anti-PTEN (1:200, Proteintech, Wuhan, China). In brief, the paraffin sections were subjected to heat-induced antigen retrieval and then incubated overnight with the primary antibody at 4°C. After rinsing, the tissue sections were incubated with horseradish peroxidase (HRP)-conjugated secondary antibody (1:200, Proteintech, Wuhan, China). Finally, all sections were incubated with DAB-Substrate (Origene, Shanghai, China) and counterstained in hematoxylin before they were dehydrated and mounted. Images were captured and analyzed using an optical microscope. The intensity of immunohistochemical staining was evaluated using a semi-quantitative grading system. The signal intensities of the positively stained tissues were analyzed using the mean integrated optical density (mean IOD) with the computer-assisted image system (Image Pro-Plus 6.0, Media Cybernetics, Bethesda, MD, USA).

2.8 siRNA and plasmid transfection

To further study the functional role of CXADR in endometriosis, we established a CXADR silencing or over-expression model in Ishikawa cell line. Pools of scrambled control or CXADR siRNA (Bochu, Changsha, China) were transfected at an end concentration of 100 nmol/L into cells using reagent (Ribobio, Guangzhou, China) according to standard protocol. An over-expression plasmid for CXADR (Fenghui Biotechnology, Changsha, China) was generated through the cloning of human CXADR cDNA into an empty pcDNA3.1 vector, and the empty vectors were used as a negative control. The over-expression plasmid

was transfected into Ishikawa cells using Lipofectamine 3 000 Reagent (Invitrogen, MA, USA).

2.9 RNA isolation and quantitative real-time PCR

To explore the effect of CXADR interference or overexpression on EMT and AKT/GSK-3 β signaling pathway *in vitro*, quantitative real-time PCR (qRT-PCR) was conducted. Total RNA was extracted from cultured cells using RNA extraction Kit (Foregene, Chengdu, China) according to the standard procedure, from which cDNA was synthesized by employing GoScriptTM Reverse Transcription System (Promega, Beijing, China). Quantitative real-time PCR was performed on an Applied Biosystem 7 300 Real-time PCR system (Biorad, California, USA) using MonAmpTM chemoHS qPCR mix (Monad, Wuhan, China). The primer sequences for real-time PCR are shown in Table 1. GAPDH was used as an internal control to quantify mRNA expression.

2.10 Western blot analysis

To explore the effect of CXADR interference or overexpression on EMT and AKT/GSK-3 β signaling pathway *in vitro*, western blot was conducted. Total protein of cells was extracted by RIPA Lysis Buffer (Beyotime Biotechnology, Shanghai, China) with protease inhibitor Phenylmethylsulfonyl fluoride (PMSF). 20 μ g of the protein was first resolved by 10% sodium dodecyl sulfate polyacrylamide gel electrophoresis, and the bands were then electro-blotted onto polyvinylidene difluoride membranes (Millipore, Shanghai, China). The membranes were blocked with 5% skim milk for 1 h and then incubated overnight at 4°C with the following primary antibodies: rabbit polyclonal

Table 1. Primers used in real-time PCR.

Gene	Forward primer	Reverse primer
CXADR	CGCTAGTCCCGAAGACCAG	CTCGTAAATGTACTCGGCCT
E-cadherin	CTTTGACGCCGAGAGCTACA	TCGACCGGTGCAATCTTCAA
Vimentin	AAGCCGAAACACCCTGCAA	CTGCAGCTCCTGGATTTCTCT
Claudin-4	CTTTGCTGCAACTGTCCACC	CCTACCCGGAACAGAGGAGA
PTEN	TGGATTGACTTAGACTTGACCT	TGCTTTGAATCCAAAAACCTTACTA
PHLPP2	CAGTGGCTTTTCCCTTCGGA	CACTCTAGCAGGTTTCGGGA
Snail	CTAGGCCCTGGCTGTACAA	GACATCTGAGTGGGTCTGGAG

anti-CXADR (1:1 000, Affinity, MI, USA), anti-E-cadherin (1:1 000, Immunoway, TX, USA), anti-vimentin (1:1 000, Immunoway, TX, USA), anti-Claudin 4 (1:2000, Abcam, Cambridge, UK), anti-phospho-AKT (1:1 000, Immunoway, TX, USA), anti-GSK-3 β (1:500, Proteintech, Wuhan, China), anti-phospho-GSK-3 β (1:1 000, Proteintech, Wuhan, China), anti-PHLPP2 (1:1 000, Immunoway, TX, USA), anti-SNAIL1 (1:1 000, Proteintech, Wuhan, China), mouse monoclonal anti-AKT (1:1 000, Immunoway, TX, USA), anti-PTEN (1:2 000, Proteintech, Wuhan, China) and anti-GAPDH (1:20 000, Proteintech, Wuhan, China). Following this, the membranes were washed three times with Tris Buffered Saline Tween-20 (TBST) and incubated with HRP-conjugated goat anti-rabbit IgG (1:5 000, Proteintech, Wuhan, China) or goat anti-mouse IgG (1:5 000, Proteintech, Wuhan, China). Signals were visualized using the enhanced chemiluminescence reagent according to the manufacturer's protocol.

2.11 Cell proliferation assay

After transfection, Ishikawa cells were seeded on 96-well flat-bottomed microplates at a density of 5 000 cells/well. The culture medium was regularly replaced. For analysis of cell proliferation, 100 μ L of Cell Counting Kit-8 (CCK-8) reagent (New Cell & Molecular, Suzhou, China) was added into each well at different time points (0 h, 24 h, 48 h), followed by incubation for 1 h at 37°C. The absorbance at 450 nm of each well was measured with a microplate reader.

2.12 Wound healing assay

After transfection, a scratch wound was made using a sterilized 10- μ l pipette tip. The cells were subsequently washed with Phosphate Buffered Saline (PBS) three times to remove cell debris. The cells were then incubated for 24 h, following which images were captured under a microscope (Olympus, Japan). Cell migration rate was calculated as $\frac{0h\ scratch\ width - 24h\ scratch\ width}{0h\ scratch\ width} \times 100\%$.

2.13 Cell invasion assay

Cell invasion assays were performed using a Transwell system (Corning, NYC, USA). After dilution with serum-free medium, 100 μ L Matrigel (cat. no. 356234; Corning, NYC, USA) was added to each transwell chamber and coagulated for 4 h at 37°C. After treatment for 48 h, Ishikawa cells were washed and cultured with serum-free medium for 12 h. Next, a 200- μ L aliquot of the above single-cell suspension (2×10^4 cells) was placed into each upper chamber of a transwell plate. The lower chamber was filled with 700 mL of medium containing 10% FBS. Medium with TGF β 1 (10 ng/mL) was also added in the lower chamber. After 24 h of incubation, the cells that invaded into the membrane were fixed in 4% formaldehyde (Solarbio, Beijing, China) for 30 min, and then stained with Gimsa (Deshi, Hangzhou, China). A cotton swab was used to remove cells remaining in the upper chamber. Images of five randomly selected fields of the fixed cells were captured, and cells were counted under a 20 \times objective lens.

2.14 Statistical analysis

All experiments were performed in triplicate. The data were expressed as means \pm standard errors of the means and analyzed by GraphPad Prism 9 (La Jolla, CA, USA). Differences between two groups were evaluated with Student's *t* tests. *P* values of less than 0.05 were considered statistically significant.

3. Results

3.1 Identification of common DEGs in three datasets

In dataset GSE7305, 431 DEGs were sifted out in total (Figure 2(a)). In dataset GSE25628, 474 DEGs were sifted out in total (Figure 2(b)). In dataset GSE58178, 62 DEGs were sifted out in total (Figure 2(c)). Common DEGs in GSE7305, GSE58178, GSE25628 were selected to form Dataset 1 (Figure 2(d)), including *AEBP1*, *CXADR* and *MME*.

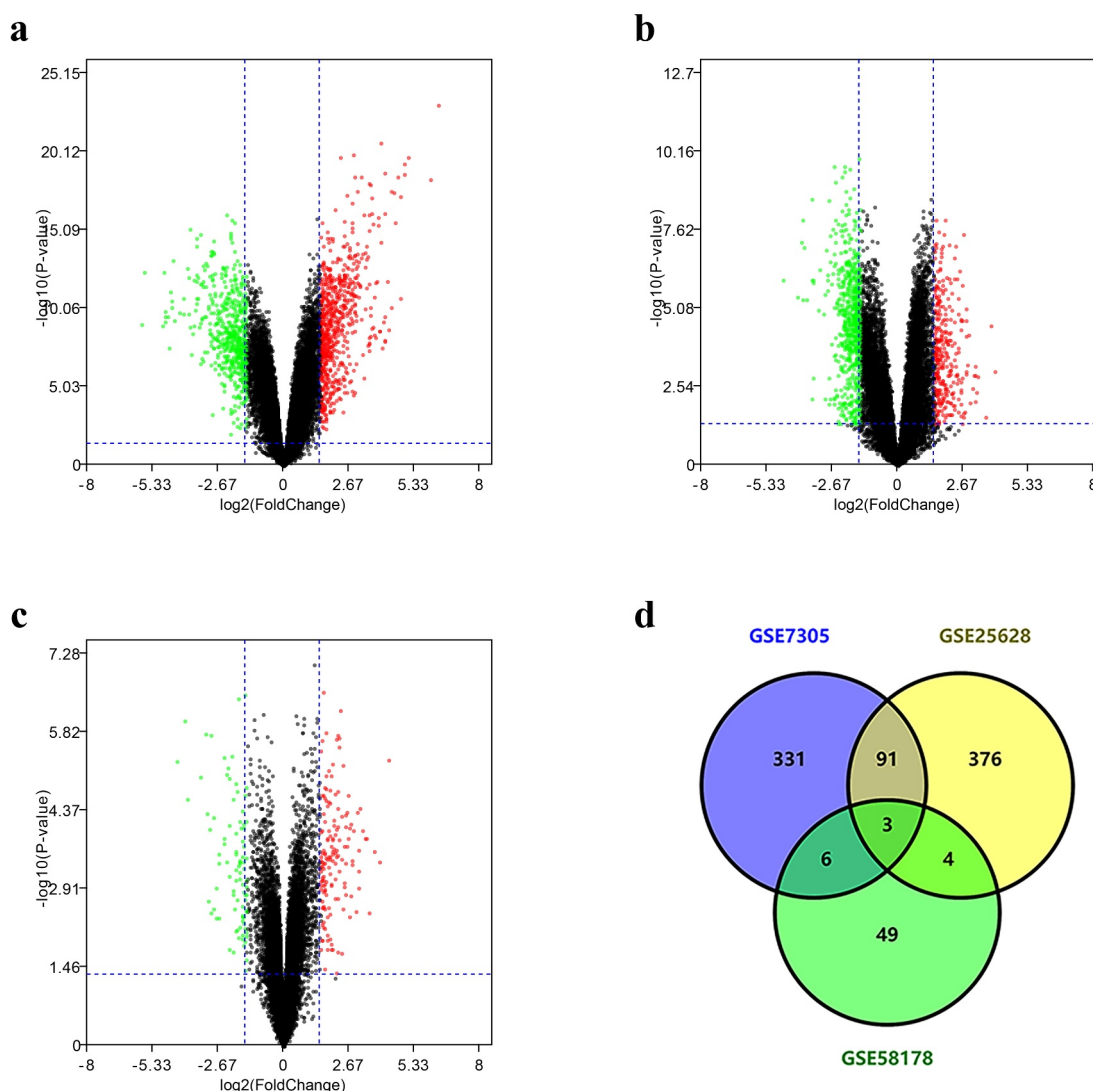


Figure 2. Identification of DEGs from the three dataset. Panel a-c shows volcano plots of DEGs between ectopic endometrium of endometriosis patients and endometrium of healthy controls in GSE7305, GSE25628 and GSE58178, respectively. Red dots represent significantly up-regulated DEGs in endometrium of endometriosis, blue dots represent significantly down-regulated DEGs in endometrium of endometriosis, gray dots indicate no significant difference. Genes satisfying the criteria $\text{adjust } P < 0.05$ and $|\log_2(\text{FC})| > 2$ were considered significant. Panel d is the venn diagram showing common DEGs among GSE7305, GSE25628 and GSE58178 (Dataset 1).

3.2 Identification of key modules and hub genes by WGCNA

We correlated modules with clinical trait and searched for the most significant associations. The results showed that module dark gray and light green were most up-regulated and down-regulated module in endometriosis compared to control in GSE7305, respectively. Module blue and brown were most up-regulated and down-regulated module in endometriosis compared to control in GSE25628, respectively. Module chocolate2 and goldenrod were most up-regulated

and down-regulated module in endometriosis compared to control in GSE58178, respectively [Figure 3\(a-c\)](#). Using a GS over 0.6 and an MM over 0.8 as cutoff criteria, 2 320, 1 618 and 1 006 genes in GSE7305, GSE25628 and GSE58178 were identified as hub genes, respectively. Common hub genes in GSE7305, GSE58178, GSE25628 were selected to form Dataset 2, and 15 hub genes were identified [Figure 3\(d\)](#). *AEBP1* and *CXADR* co-existed in Dataset 1 and Dataset 2 [Figure 3\(e\)](#), but the association between *AEBP1* and endometriosis has been reported [26]. We therefore selected *CXADR*, which was down-

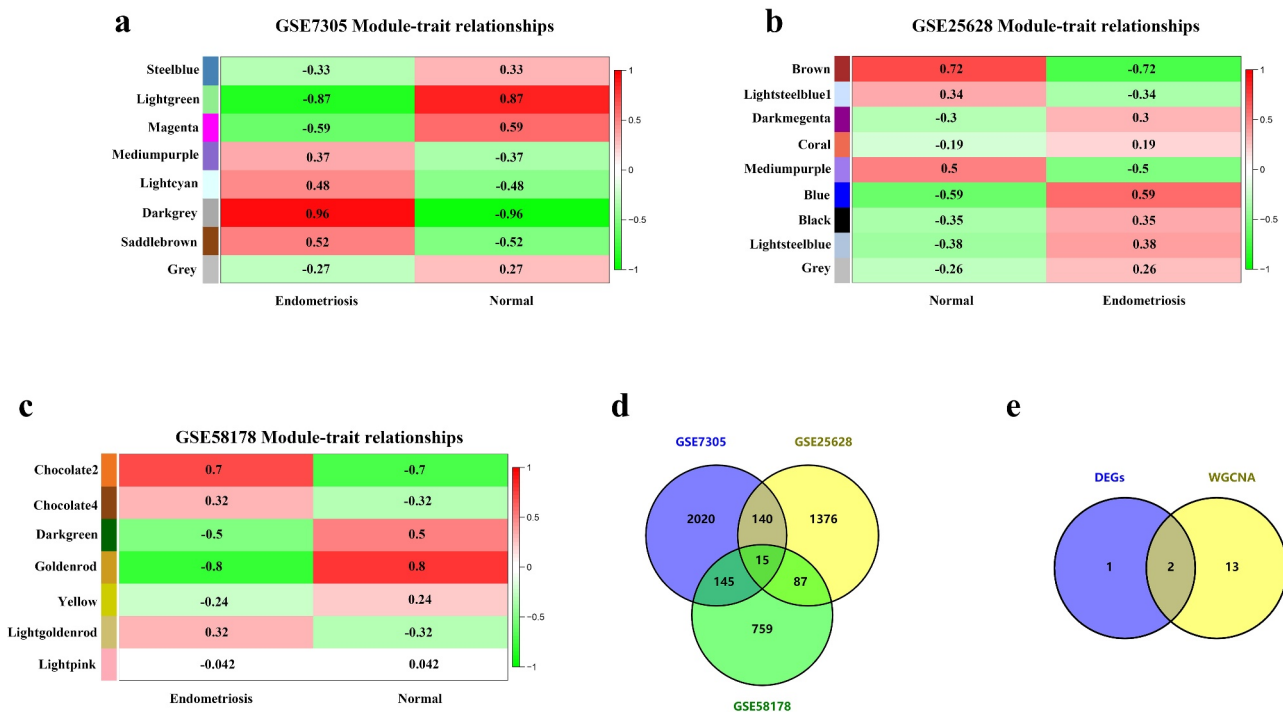


Figure 3. Weighted gene co-expression network analysis of genes in endometriosis. Panel a-c shows analysis of module-trait relationships of endometriosis. Each row represents a module eigengene, and each column represents a trait. Genes clusters (modules) were displayed in different colors. In each module, red and green blocks represents positive and negative correlation with the trait, respectively. The higher the absolute value of the number in the module, the more relevant the module is to the trait. Panel d is the venn diagram showing the common hub genes among GSE7305, GSE25628 and GSE58178 (Dataset 2). Panel e is the venn diagram showing common genes between the Dataset 1 and Dataset 2.

regulated in ectopic endometrium compared with that in the normal endometrium, as the final key gene.

3.3 Verification the trends of CXADR, PTEN, PHLPP2, SNAIL1, E-cadherin, vimentin and Claudin-4 in endometriosis by IHC

IHC analysis showed that CXADR, PHLPP2, PTEN, E-cadherin, Claudin-4 expression was significantly decreased in ovarian endometriotic tissue compared with that in controls, while SNAIL1 and vimentin was significantly increased in ovarian endometriotic tissue compared with that in controls Figure 4(a-h). Yanira et al. reported expression of AKT and GSK3 β was identical in endometriotic samples and controls, whereas p-AKT and p-GSK3 β remained over-expressed in endometriosis [27]. However, their results were

solely based on immunohistochemistry stain data, and functional experiments were lacked.

3.4 CXADR regulates cell proliferation, migration and invasion *in vitro*

To identify whether CXADR affected the biological behaviors of endometrial cells, the endometrial cell-line Ishikawa was transfected with cDNA containing CXADR and its negative control (NC) for 48 h. The level of CXADR increased significantly after transfection Figure 5(a), which confirmed that the transfection was effective. To evaluate the effect of CXADR on cell viability, we performed CCK-8 assay on Ishikawa cell line after transfected with CXADR cDNA or NC. The results indicated that CXADR significantly suppressed cell viability Figure 5(b). We further performed transwell on cell line to evaluate the

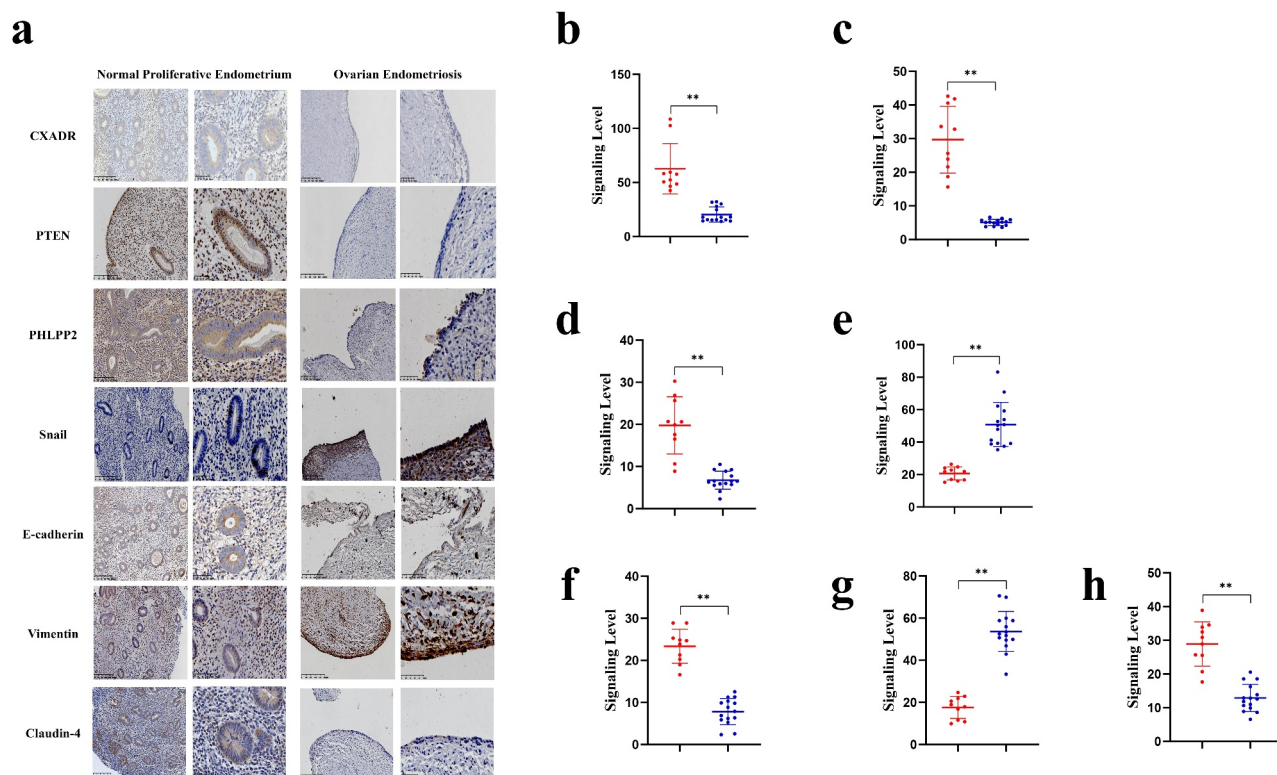


Figure 4. Abnormal CXADR, PHLPP2, PTEN, SNAIL1, E-cadherin, vimentin and claudin-4 expression were observed in endometriosis. Panel a shows immunohistochemical analysis of the expression of CXADR, PTEN, PHLPP2, SNAIL1, E-cadherin, vimentin and claudin-4 in endometrium of controls and ovarian endometriosis. Panel b-h shows mean IOD of the expression of CXADR, PTEN, PHLPP2, SNAIL1, E-cadherin, vimentin and claudin-4 respectively. Each dot refers to mean IOD in each section. The data were expressed as means \pm standard errors of the means (** $P < 0.01$).

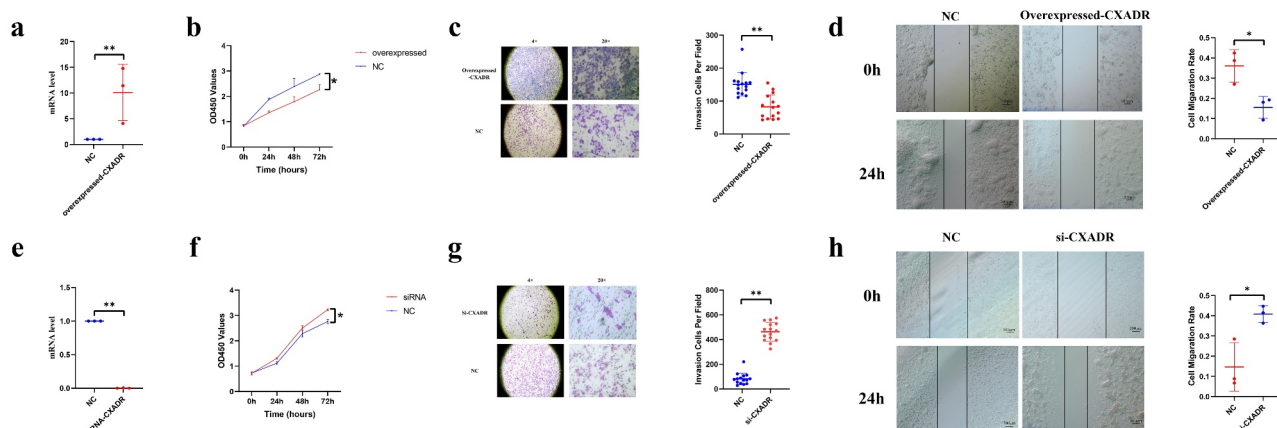


Figure 5. CXADR regulates cell proliferation, migration and invasion *in vitro*. Panel a and e shows the mRNA level of CXADR after transfected with cDNA containing CXADR or si-CXADR, respectively. Each dot refers to an independent experiment. Panel b and f shows CCK-8 assay of the viability of Ishikawa cells after transfected with cDNA containing CXADR or si-CXADR, respectively. Panel c and g shows transwell assay evaluating the invasion of Ishikawa cells after transfected with cDNA containing CXADR or si-CXADR, respectively. Photographs were taken at 4 \times or 20 \times magnification. Scale bars represent 500 μ m and 100 μ m, respectively. Each dot refers to one field of the fixed cells counted under a 20 \times objective lens. Panel d and h shows wound assay of Ishikawa cells after transfected with cDNA containing CXADR or si-CXADR, respectively. Each dot refers to an independent experiment. Scale bars represent 200 μ m. All experiments were performed in triplicate. The data were expressed as means \pm standard errors of the means (* $P < 0.05$, ** $P < 0.01$).

effect of CXADR on cell invasion. The results indicated that CXADR inhibited cell invasion in Ishikawa cell lines, and the difference was statistically significant [Figure 5\(c\)](#). Wound healing assay also showed that CXADR inhibited cell migration significantly [Figure 5\(d\)](#).

We further transfected Ishikawa cell line with CXADR siRNA and inhibitor NC to see whether CXADR down-regulation had the opposite effects with CXADR over-expression. The transfection efficiency was verified by qRT-PCR [Figure 5\(e\)](#). CCK-8 assay showed that inhibiting CXADR promoted endometrial cell viability [Figure 5\(f\)](#). Transwell showed that the down-regulation of CXADR significantly increased the cell invasion ability [Figure 5\(g\)](#). Wound healing results showed that CXADR down-regulation could promote cell migration significantly [Figure 5\(h\)](#).

3.5 CXADR regulates EMT progression in Ishikawa cells by controlling AKT signaling pathway

To gain insight into the mechanisms underlying the function of CXADR in Ishikawa cell line, the expression of the AKT/GSK-3 β signaling pathway and EMT markers in Ishikawa cells transfected with plasmid carrying a CXADR cDNA or CXADR siRNA were analyzed. The qRT-PCR and western blot results indicated the significantly increased expression of vimentin, and decreased expression of E-cadherin and Claudin 4 in the presence of the CXADR siRNA. In addition, we detected significantly decreased levels of PTEN and PHLPP2, and significantly increased level of SNAIL1 in CXADR knockdown compared with control. The levels of phosphorylated AKT (p-AKT), phosphorylated GSK-3 β (p-GSK-3 β) were also increased in CXADR knockdown compared with control cells [Figure 6\(a,b\)](#).

Conversely, CXADR over-expression had the opposite effects with CXADR down-regulation. The results indicated significantly decreased expression of vimentin, and increased expression of E-cadherin and Claudin 4 in the presence of the CXADR over-

expression. The levels of PTEN and PHLPP2 were significantly increased in CXADR over-expression compared with control. The levels of p-AKT, p-GSK-3 β and SNAIL1 were decreased, in CXADR over-expression compared with control cells [Figure 6\(c,d\)](#).

4. Discussion

Increasing evidence suggests that the endometrium obtained endometriosis exhibits abnormal molecular expression, which boost the endometrium to invade and implant into other organs, such as ovary [13]. In this context, combined with *in silico* and *in vitro* study, we identified CXADR as a potential driver in endometriosis.

Previous study identified CXADR as a critical regulator of EMT in breast cancer [12], while we first showed that CXADR may also play an important role in endometriosis. To further investigate the influence of CXADR dysregulation on endometrial epithelial cell activities, a series of functional assays were conducted in Ishikawa cells. The results demonstrated that knockdown of CXADR promoted cell proliferation, migration, and invasion, whereas over-expression of CXADR inhibited these cellular bioactivities. Concomitantly, knockdown of CXADR increased the protein expression of vimentin but decreased the expression of E-cadherin. Therefore, CXADR may exhibit oncogene-like properties in endometriosis by regulating the EMT process.

Importantly, EMT is activated when interacting with extracellular matrix components and soluble growth factors, such as TGF- β family members [25,28]. TGF- β -mediated EMT therefore plays a significant role in facilitating cell metastasis and invasion [29]. However, previous studies focused mainly on TGF- β /smad signaling pathway [30], the exact role of TGF- β -mediated AKT/GSK-3 β signaling pathway in endometriosis was unclear, except that Yanira et al. reported expression of AKT and GSK3 β was identical in endometriotic samples and controls, whereas p-AKT and p-GSK3 β remained over-expressed in endometriosis [27]. However, their results were solely based on immunohistochemistry stain data, and functional experiments were lacked. In

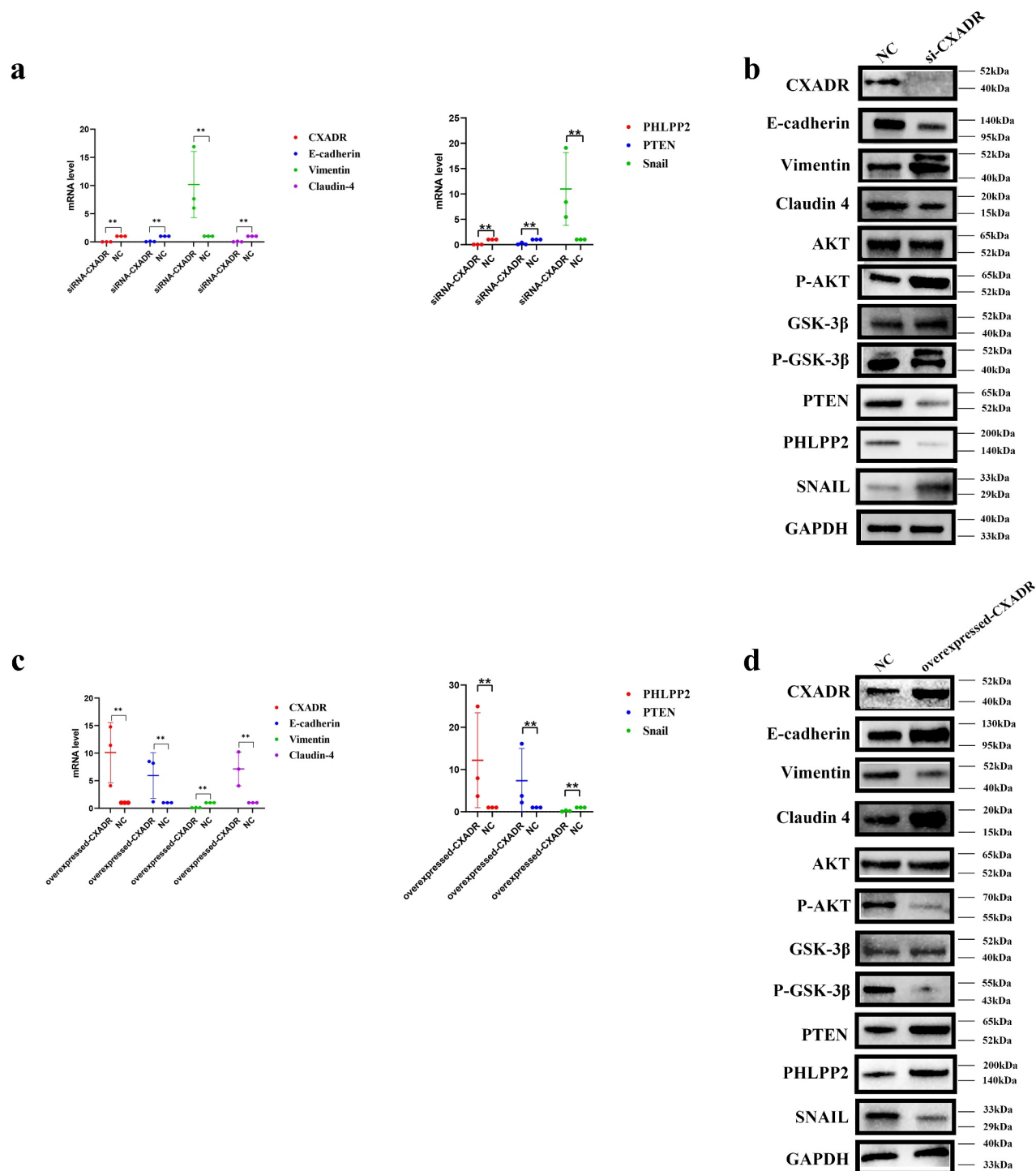


Figure 6. CXADR regulates EMT progression in Ishikawa cells by controlling AKT/GSK 3 β signaling pathway. Panel a and c shows the mRNA level of CXADR, E-cadherin, vimentin, claudin-4, PHLPP2, PTEN and SNAIL1 in Ishikawa cells after transfected with si-CXADR or cDNA containing CXADR, respectively. Each dot refers to an independent experiment. Panel b and d shows protein expression of E-cadherin, vimentin, claudin-4, AKT, p-AKT, GSK-3 β , p-GSK-3 β , PTEN, PHLPP2 and SNAIL1 in Ishikawa cells after transfected with si-CXADR or cDNA containing CXADR, respectively. All experiments were performed in triplicate. The data were expressed as means \pm standard errors of the means (** $P < 0.01$).

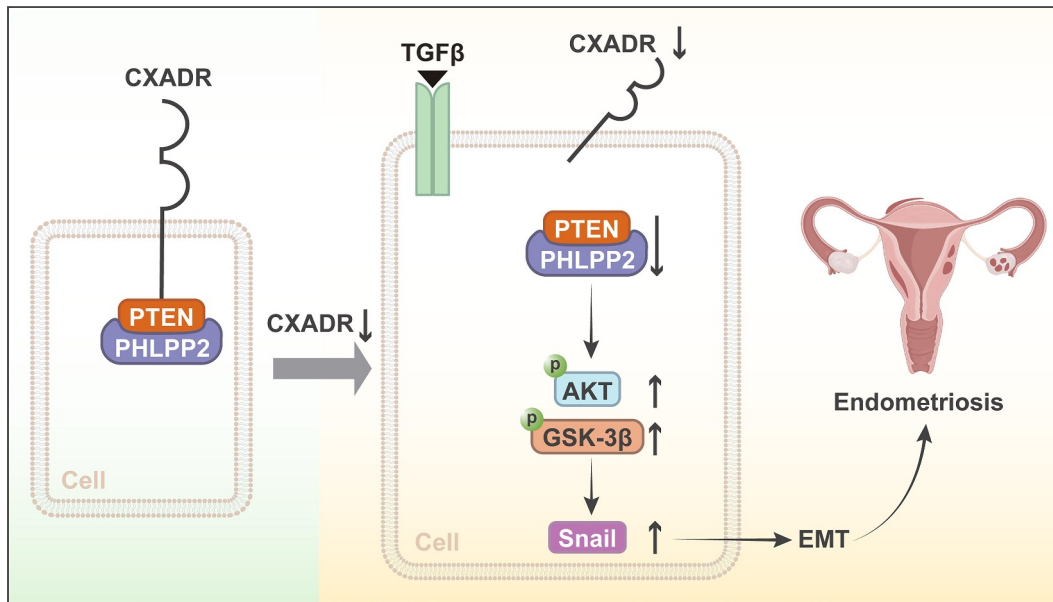


Figure 7. Mechanistic diagrams. CXADR controls epithelial–mesenchymal transition (EMT) in endometriosis by stabilizing the AKT regulators PTEN and PHLPP2.

present study, through comprehensive *in vitro* experiments, we suggested that TGF- β -mediated AKT/GSK-3 β signaling pathway, with CXADR a leading role in controlling, may be another TGF- β -mediated signaling pathway to promote EMT in endometriosis. CXADR, PHLPP2 and PTEN expression were significantly decreased in ovarian endometriotic tissue compared with that in controls, while SNAIL1 was significantly increased in ovarian endometriotic tissue compared with that in controls. In Ishikawa cell line, loss of CXADR resulted in loss of PHLPP2 and PTEN, phosphorylation of AKT and GSK3 β , and thus sensitized cells to TGF- β -induced EMT (Figure 7). A weakness of this study is Ishikawa cells were used instead of primary endometrial epithelial cells for transfection.

Epigenetic aberrations are involved in the pathogenesis of endometriosis [31,32], of which histone acetylation is the best studied form of epigenetic modification [31]. The balance between histone acetyltransferases and histone deacetylases (HDACs) controls the acetylation levels of histone [32]. Histone acetyltransferases transfer acetyl groups from acetyl-coenzyme A to lysine residues on the aminoterminal region of histones, and they activate genetic transcription. Conversely, HDACs, which target promoter sites through sequence-specific transcription, remove the acetyl

groups and prevent transcription [33]. Valproic acid (VPA), a kind of histone deacetylases inhibitors (HDACi), can prevent the transcriptional-inhibiting effects of HDAC. Our bioinformatics analysis showed CXADR was a VPA-targeted gene that were up-regulated by VPA treatment, indicating the cause of CXADR down-regulation is epigenetic aberrations (See Supplementary). In addition, these findings also suggested that HDACi are promising agents for the treatment of endometriosis.

Endometriosis creates a significant clinical and economic burden on young women and society [5,6]. Therefore, the utility of resources and researches need to be maximized to enhance our understanding of the disease and to develop novel and effective treatments. At present, there is still a lot of mining space in publicly available data sets. This study also emphasized *in silico* combined with confirmatory “wet lab” data may provide new ideas on pathogenesis and find new promising therapeutic targets for not limited to endometriosis.

In conclusion, our research identified CXADR as a novel driver of EMT, via the AKT/GSK-3 β signaling axis, in endometriosis. Further detailed studies, such as animal models and clinical trials, of the mechanisms and functions of CXADR in endometriosis are needed.

Disclosure statement

No potential conflict of interest was reported by the author(s).

Funding

This research was funded by the National Key R&D Program of China [2017YFC1001100].

Author contribution statement

HJ-T and HM-X performed study concept and design; HJ-T, ZH-D and HW-D performed development of methodology and writing, review and revision of the paper; CZ provided acquisition, analysis and interpretation of data, and statistical analysis. All authors read and approved the final paper.

Data availability statement

The data that support the findings of this study are openly available in Gene Expression Omnibus (GEO) database (<https://www.ncbi.nlm.nih.gov/geo>). All data generated or analyzed during this study are included in this article. Further enquiries can be directed to the corresponding author.

Ethics statement

This study was approved by the Ethics Committees of School of basic medicine, Central South University (2022-KT109), and written informed consent was obtained from all patients before surgical procedures and sample collection.

References

- [1] Giudice LC. Clinical practice endometriosis. *N Engl J Med.* 2010 Jun 24;362(25):2389–2398.
- [2] Borghese B, Zondervan KT, Abrao MS, et al. Recent insights on the genetics and epigenetics of endometriosis. *Clin Genet.* 2017 Feb 1;91(2):254–264.
- [3] Shafrir AL, Farland LV, Shah DK, et al. Risk for and consequences of endometriosis: a critical epidemiologic review. *Best Pract Res Clin Obstet Gynaecol.* 2018 Aug 1;51:1–15.
- [4] Tomassetti C, D’Hooghe T. Endometriosis and infertility: insights into the causal link and management strategies. *Best Pract Res Clin Obstet Gynaecol.* 2018 Aug 1;51:25–33. doi: [10.1016/j.bpobgyn.2018.06.002](https://doi.org/10.1016/j.bpobgyn.2018.06.002)
- [5] Flores I, Rivera E, Ruiz LA, et al. Molecular profiling of experimental endometriosis identified gene expression patterns in common with human disease. *Fertil Steril.* 2007 May 1;87(5):1180–1199.
- [6] Van Gorp T, Amant F, Neven P, et al. Endometriosis and the development of malignant tumours of the

- pelvis. A review of literature. *Best Pract Res Clin Obstet Gynaecol.* 2004 Apr 1;18(2):349–371.
- [7] Sampson JA. Metastatic or embolic endometriosis, due to the menstrual dissemination of endometrial tissue into the venous circulation. *Am J Pathol.* 1927 Mar 1;3(2):93–110.
- [8] Hull ML, Nisenblat V. Tissue and circulating microRNA influence reproductive function in endometrial disease. *Reprod Biomed Online.* 2013 Nov 1;27(5):515–529.
- [9] Zhang Y, Wang S, Li D, et al. A systems biology-based classifier for hepatocellular carcinoma diagnosis. *PLOS ONE.* 2011 Jan 20;6(7):e22426. doi: [10.1371/journal.pone.0022426](https://doi.org/10.1371/journal.pone.0022426)
- [10] O’Neill MC, Song L. Neural network analysis of lymphoma microarray data: prognosis and diagnosis near-perfect. *BMC Bioinform.* 2003 Apr 10;4(1):13.
- [11] Singaraju S, Prasad H, Singaraju M. Evolution of dental informatics as a major research tool in oral pathology. *J Oral Maxillofac Pathol.* 2012 Jan 1;16(1):83–87.
- [12] Nilchian A, Johansson J, Ghalali A, et al. CXADR-mediated formation of an AKT inhibitory signalosome at tight junctions controls epithelial–mesenchymal plasticity in breast cancer. *Cancer Res.* 2019 Jan 1;79(1):47–60. doi: [10.1158/0008-5472.CAN-18-1742](https://doi.org/10.1158/0008-5472.CAN-18-1742)
- [13] Balda MS, Matter K. Tight junctions as regulators of tissue remodelling. *Curr Opin Cell Biol.* 2016 Oct 1;42:94–101. doi: [10.1016/j.ceb.2016.05.006](https://doi.org/10.1016/j.ceb.2016.05.006)
- [14] Konrad L, Dietze R, Riaz MA, et al. Epithelial–mesenchymal transition in endometriosis—when does it happen? *JCM.* 2020 Jun 18;9(6):1915. doi: [10.3390/jcm9061915](https://doi.org/10.3390/jcm9061915)
- [15] Chaffer CL, San JB, Lim E, et al. EMT, cell plasticity and metastasis. *Cancer Metastasis Rev.* 2016 Dec 1;35(4):645–654.
- [16] Nieto MA. Epithelial plasticity: a common theme in embryonic and cancer cells. *Science.* 2013 Nov 8;342(6159):1234850.
- [17] Bartley J, Julicher A, Hotz B, et al. Epithelial to mesenchymal transition (EMT) seems to be regulated differently in endometriosis and the endometrium. *Arch Gynecol Obstet.* 2014 Apr 1;289(4):871–881.
- [18] Proestling K, Birner P, Gamperl S, et al. Enhanced epithelial to mesenchymal transition (EMT) and upregulated MYC in ectopic lesions contribute independently to endometriosis. *Reprod Biol Endocrinol.* 2015 Jul 22;13(1):75. doi: [10.1186/s12958-015-0063-7](https://doi.org/10.1186/s12958-015-0063-7)
- [19] Hever A, Roth RB, Hevezi P, et al. Human endometriosis is associated with plasma cells and overexpression of B lymphocyte stimulator. *Proc Natl Acad Sci, USA.* 2007 Jul 24;104(30):12451–12456. doi: [10.1073/pnas.0703451104](https://doi.org/10.1073/pnas.0703451104)
- [20] Monsivais D, Dyson MT, Yin P, et al. ER β - and prostaglandin E2-regulated pathways integrate cell proliferation via Ras-like and estrogen-regulated growth inhibitor in endometriosis. *Mol Endocrinol.* 2014 Aug 1;28(8):1304–1315. doi: [10.1210/me.2013-1421](https://doi.org/10.1210/me.2013-1421)
- [21] Crispi S, Piccolo MT, D’Avino A, et al. Transcriptional profiling of endometriosis tissues identifies genes

- related to organogenesis defects. *J Cell Physiol.* **2013** Sep 1;228(9):1927–1934. doi: [10.1002/jcp.24358](https://doi.org/10.1002/jcp.24358)
- [22] Langfelder P, Horvath S. WGCNA: an R package for weighted correlation network analysis. *BMC Bioinform.* **2008** Dec 29;9(1):559.
- [23] Long J, Huang S, Bai Y, et al. Transcriptional landscape of cholangiocarcinoma revealed by weighted gene coexpression network analysis. *Brief Bioinform.* **2021** Jul 20;22(4). doi: [10.1093/bib/bbaa224](https://doi.org/10.1093/bib/bbaa224)
- [24] Tang J, Yang Q, Cui Q, et al. Weighted gene correlation network analysis identifies RSAD2, HERC5, and CCL8 as prognostic candidates for breast cancer. *J Cell Physiol.* **2020** Jan 1;235(1):394–407. doi: [10.1002/jcp.28980](https://doi.org/10.1002/jcp.28980)
- [25] Matsuzaki S, Darcha C. Epithelial to mesenchymal transition-like and mesenchymal to epithelial transition-like processes might be involved in the pathogenesis of pelvic endometriosis. *Hum Reprod.* **2012** Mar 1;27(3):712–721.
- [26] Bakhtiarizadeh MR, Hosseinpour B, Shahhoseini M, et al. Weighted gene co-expression network analysis of endometriosis and Identification of functional modules associated with its main hallmarks. *Front Genet.* **2018** Jan 20;9:453. doi: [10.3389/fgene.2018.00453](https://doi.org/10.3389/fgene.2018.00453)
- [27] Franco-Murillo Y, Miranda-Rodriguez JA, Rendon-Huerta E, et al. Unremitting cell proliferation in the secretory phase of eutopic endometriosis: involvement of pAkt and pGsk3 β . *Reprod Sci.* **2015** Apr 1;22(4):502–510. doi: [10.1177/1933719114549843](https://doi.org/10.1177/1933719114549843)
- [28] Thiery JP, Sleeman JP. Complex networks orchestrate epithelial-mesenchymal transitions. *Nat Rev Mol Cell Biol.* **2006** Feb 1;7(2):131–142.
- [29] Budi EH, Duan D, Derynck R. Transforming growth factor- β receptors and smads: regulatory complexity and functional versatility. *Trends Cell Biol.* **2017** Sep 1;27(9):658–672.
- [30] Wang S, Zhang M, Zhang T, et al. microRNA-141 inhibits TGF-beta1-induced epithelial-to-mesenchymal transition through inhibition of the TGF-beta1/SMAD2 signalling pathway in endometriosis. *Arch Gynecol Obstet.* **2020** Mar 1;301(3):707–714.
- [31] Kawano Y, Nasu K, Li H, et al. Application of the histone deacetylase inhibitors for the treatment of endometriosis: histone modifications as pathogenesis and novel therapeutic target. *Hum Reprod.* **2011** Sep 1;26(9):2486–2498. doi: [10.1093/humrep/der203](https://doi.org/10.1093/humrep/der203)
- [32] Abe W, Nasu K, Nakada C, et al. miR-196b targets c-myc and bcl-2 expression, inhibits proliferation and induces apoptosis in endometriotic stromal cells. *Hum Reprod.* **2013** Mar 1;28(3):750–761.
- [33] Pazin MJ, Kadonaga JT. What's up and down with histone deacetylation and transcription? *Cell.* **1997** May 2;89(3):325–328.